

## RESEARCH ARTICLE

10.1002/2017JB014777

## Key Points:

- Seventeen mud volcanoes (of which five are newly formed) erupted during the 2016–17 Central Italy seismic sequence after major earthquakes
- We investigate how dynamic and static stresses, from the three main earthquakes, influence mud volcano eruptions
- Static stress changes (−0.44 to 0 bar) did not influence eruptions, which were triggered by transient dynamic stresses (up to ~3.9 bar)

## Supporting Information:

- Supporting Information S1
- Table S1
- Table S2

## Correspondence to:

D. Maestrelli,  
daniele.maestrelli@for.unipi.it

## Citation:

Maestrelli, D., Bonini, M., Delle Donne, D., Manga, M., Piccardi, L., & Sani, F. (2017). Dynamic triggering of mud volcano eruptions during the 2016–2017 Central Italy seismic sequence. *Journal of Geophysical Research: Solid Earth*, 122. <https://doi.org/10.1002/2017JB014777>

Received 25 JUL 2017

Accepted 28 OCT 2017

Accepted article online 2 NOV 2017

## Dynamic Triggering of Mud Volcano Eruptions During the 2016–2017 Central Italy Seismic Sequence

Daniele Maestrelli<sup>1,2</sup> , Marco Bonini<sup>3</sup> , Dario Delle Donne<sup>4</sup> , Michael Manga<sup>5</sup> , Luigi Piccardi<sup>3</sup>, and Federico Sani<sup>2,3</sup>

<sup>1</sup>Dipartimento di Scienze della Terra, Università di Pisa, Pisa, Italy, <sup>2</sup>Dipartimento di Scienze della Terra, Università di Firenze, Firenze, Italy, <sup>3</sup>Istituto di Geoscienze e Georisorse, Consiglio Nazionale delle Ricerche, Firenze, Italy, <sup>4</sup>Dipartimento di Scienze della Terra e del Mare, Università di Palermo, Palermo, Italy, <sup>5</sup>Department of Earth and Planetary Science, University of California, Berkeley, CA, USA

**Abstract** On 24 August 2016 a seismic event ( $M_w$  6.0) was the first of the long Central Italy sequence (ongoing at the end of 2017) of medium-to-high magnitude earthquakes, with nine  $M_w \geq 5$  up to October 2017, and with about 74,000 seismic events registered after 1 year. The largest was the  $M_w$  6.5 30 October 2016 event near Norcia. After the major seismic events, 17 mud volcanoes erupted around Monteleone di Fermo village (Marche region). Mud volcano eruptions generally occurred a few hours to a few days after the main earthquakes, suggesting a seismic triggering. We analyzed the peak ground velocities and dynamic stresses during the three largest earthquakes. We also evaluated the static stress changes in order to assess the potential influence of normal stress changes on the feeder system of the activated mud volcanoes. We find a correlation with dynamic stresses, whereas static stress changes are negligible or negative (with values reaching −0.44 bar, clamping feeder dykes). We conclude that seismic shaking (up to ~3.9 bar during Norcia earthquake) is the dominant driver for these eruptions. Finally, we evaluated the response ratio as a function of the dynamic stress. It increases exponentially with peak dynamic stress varying from <10% for peak dynamic stress >0.3 bar to >50% for peak dynamic stress >2 bar, indicating a link between earthquake shaking and mud volcano activity.

### 1. Introduction and Aims of the Study

A strong seismic sequence ( $M_{w,max} = 6.5$ ) struck Central Italy starting on 24 August 2016 (Chiaraluce et al., 2017; Livio et al., 2016; Tinti et al., 2016; Cheloni et al., 2017). These earthquakes were accompanied by collateral effects, among which the eruption of mud volcanoes.

Mud volcanoes and fluid seeps are widely distributed along the eastern thrust fronts of the Italian peninsula (Martinelli & Judd, 2004). The term mud volcanism includes a series of similar phenomena, which share in common the emission of a mud/water mixture at surface. Different processes can lead to these manifestations, spanning from the overpressure induced by the presence of gaseous fluids (e.g., hydrocarbon) as additional phase in the mixture to processes related to the upward migration of geothermal fluids or simply to density contrasts (Kopf, 2002). Whatever the process, they can be categorized according to morphological features (e.g., Kopf, 2002; Planke et al., 2003). Collapsed features are commonly called mud pools, or salsas, while mud extrusion leading in the formation of conical edifices are classified on the basis of their height: gryphons (less than 3 m tall), mud cones (3 to 10 m in height), and mud volcanoes (up to 400 m tall for onshore edifices). For simplicity, herein we generically use the term mud volcano (MV), but strictly speaking the features that we are going to describe are mud pool and gryphons, the extrusive features being never taller than 3 m. From a genetic point of view, no anomalous geothermal gradient is reported at the emission points, and mud volcanism is likely related to the ascent of cold fluids driven by gas-induced overpressures, as is the case of the well-known mud volcanoes along the Pede-Apennine margin of the Northern Apennine (Emilia-Romagna). Their eruptions have been described since 91 Before Common Era by the Roman writer Plinius in his *Naturalis Historia*, and more recently by others (e.g., Bonini, 2009; Manga & Bonini, 2012). Seismic triggering of mud volcanoes is a phenomenon well documented worldwide (Manga & Brodsky, 2006; Mellors et al., 2007). Whereas the Emilia-Romagna mud volcanoes have been widely studied (e.g., Bonini, 2008; Capozzi & Picotti, 2002, 2010; Lupi et al., 2015; Oppo et al., 2013), less documented are the geological and historical activities of mud volcanoes in Central Italy. In this region, all along the Marche and the Abruzzo Apennine

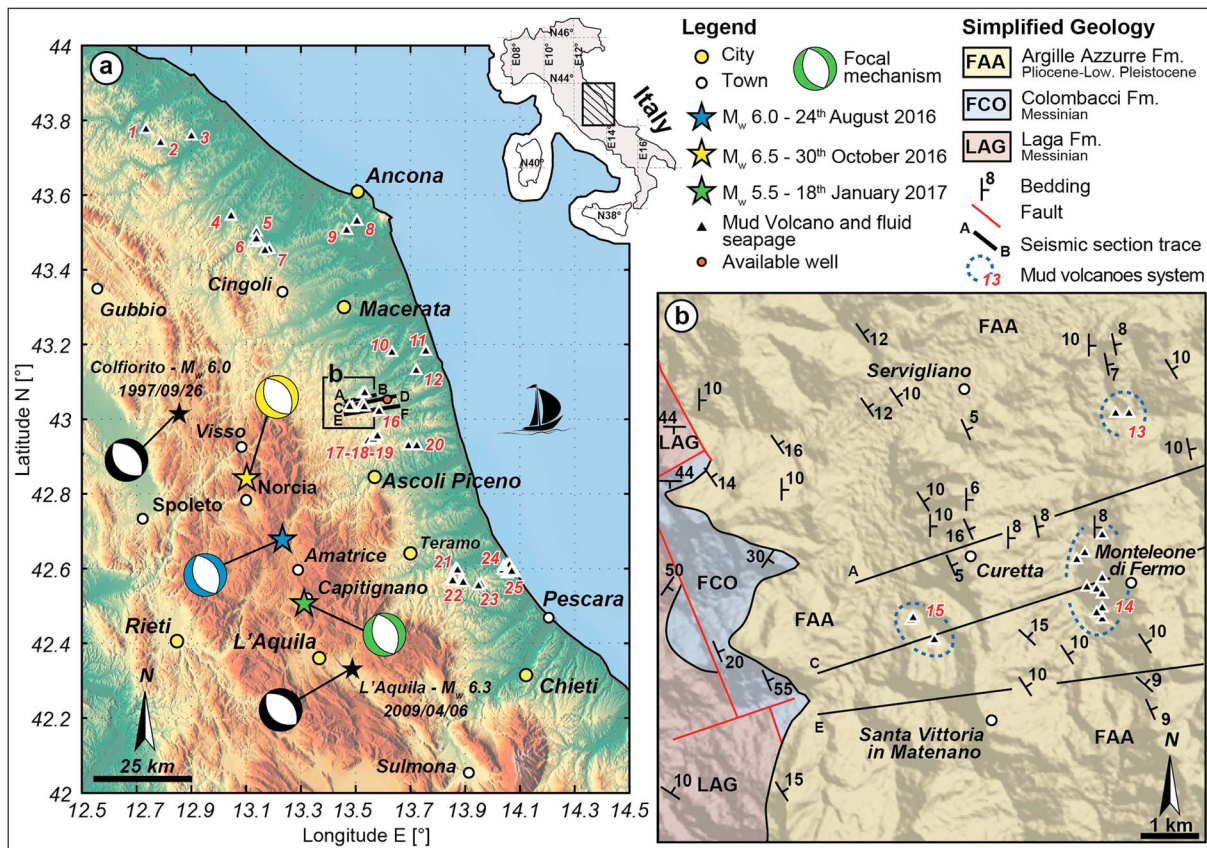


**Figure 1.** (a) Epicenters of the main seismic events that hit Central Italy during the two last decades (after INGV catalogue; <http://cnt.rm.ingv.it>); mud volcanoes are also shown. (b) Detail of geological setting of the Monteleone di Fermo area (simplified from the CARG 1:10.000 geological map, available on the Marche cartographic archive at <http://www.ambiente.marche.it/>), where several mud volcanoes were activated after the major earthquakes of 24 August and 30 October 2016. The red numbers refers to mud volcano systems reported in Table S1. Focal mechanisms are available at <http://info.terremoti.ingv.it/>. The colored focal mechanism refers to the seismic events investigated in this study.

foothills, emission of saline water and mixtures of mud and hydrocarbons occur at fractures and at small mud volcanoes (Bonasera, 1952, 1954; Damiani, 1964).

Here we focus on the Monteleone di Fermo area (Fermo Province) in the Marche region, where 17 mud volcanoes (out of about 80 in the whole region) erupted (some of them with multiple paroxysmal episodes) shortly after the major earthquakes of the 2016–2017 Central Italy seismic sequence (Figure 1 and Tables 1 and 2). The background quiescent activity of mud volcanoes generally consists of the quiet and intermittent

flow of mud and fluids, which is often featured by gas bubbles popping up through the muddy water. The paroxysmal activity that followed the 2016 earthquakes consisted in the dramatic increase of fluid and mud discharge, sometimes with the mud thrown up in the air, as well as the formation of new vents, or the reactivation of inactive seeps.

The epicenters are quite far from the mud volcanoes that erupted at Monteleone di Fermo, the latter being located at an epicentral distance  $\geq 40$  km (Figure 1). Nonetheless, an impressive series of eruptions occurred from few hours up to 1–2 days after the main shocks, suggesting a correlation between the seismic events and the mud emissions. In some intriguing cases, the investigated mud volcanoes were not present before the earthquake, but formed immediately after (e.g., a new mud volcano, hereafter called Contrada S. Lazzaro MV, formed 28 h after the  $M_w$  6.5 Norcia earthquake of 30 October 2016). These occurrences are indeed anomalous. As an example, the so-called S.M. in

**Table 1**  
Major Seismic Events of the Central Italy Seismic Sequence, Which Started on 24 August 2016 and Is Still Ongoing

Date	Time (UTC)	$M_w$	Lat. N (deg)	Long. E (deg)	Depth (km)
<b>24/8/2016</b>	<b>01:36:32</b>	<b>6.0</b>	<b>42.698300</b>	<b>13.233500</b>	<b>8.1</b>
24/8/2016	02:33:28	5.4	42.792200	13.150700	8.0
26/10/2016	17:10:36	5.4	42.880200	13.127500	8.7
26/10/2016	19:18:05	5.9	42.908700	13.128800	7.5
<b>30/10/2016</b>	<b>06:40:17</b>	<b>6.5</b>	<b>42.832200</b>	<b>13.110700</b>	<b>9.2</b>
18/1/2017	09:25:40	5.1	42.546800	13.262300	9.2
<b>18/1/2017</b>	<b>10:14:19</b>	<b>5.5</b>	<b>42.529300</b>	<b>13.282300</b>	<b>9.0</b>
18/1/2017	10:25:23	5.4	42.494300	13.311200	8.9
18/1/2017	13:33:36	5.0	42.477300	13.280700	10.0

Note. The three events marked in bold are those considered in our study (data from INGV catalogue available at <http://cnt.rm.ingv.it/>).

**Table 2**  
Mud Volcanoes That Erupted After the Three Major Seismic Events Considered in This Study

MV name	Postseismic paroxysmal activity	PGV(cm/s)	Min. dynamic stress (bar)	Max. dynamic stress (bar)
<b><i>M<sub>w</sub> 6.0 on 24 August 2016 01:36:32 (UTC)</i></b>				
S.Maria in Paganico	24 August	6.30	1.06	2.72
La Croce	Early postseismic event <sup>a</sup>	7.34	1.23	3.17
Case tedeschi 2 bis	24–26 August	7.34	1.23	3.17
<b><i>M<sub>w</sub> 6.5 on 30 October 2016 06:40:17 (UTC)</i></b>				
S.Maria in Paganico	30 October, 12.00 a.m.–6.00 p.m. (UTC)	5.62	0.94	2.43
Valle Corvone	30 October	6.41	1.08	2.77
Valle Corvone bis	30 October	6.41	1.08	2.77
La Croce	Early postseismic event <sup>a</sup>	6.36	1.07	2.75
Monteleone 1	Early postseismic event <sup>a</sup>	6.23	1.05	2.69
Monteleone 2	Early postseismic event <sup>a</sup>	6.20	1.04	2.68
Monteleone 3	Early postseismic event <sup>a</sup>	6.20	1.04	2.68
Case Tedeschi 1	Early postseismic event <sup>a</sup>	6.26	1.05	2.70
Case Tedeschi 1 Bis	Early postseismic event <sup>a</sup>	6.25	1.05	2.70
Case Tedeschi 3	Early postseismic event <sup>a</sup>	6.22	1.05	2.69
Case Tedeschi 3 Bis	Early postseismic event <sup>a</sup>	6.23	1.05	2.69
Contrada S. Salvatore 1	1 November	8.76	1.47	3.78
Contrada S. Salvatore 2	1 November, 11.00 a.m. (UTC)	9.01	1.51	3.89
Contrada S. Salvatore 3	1 November	8.97	1.51	3.88
Vallocchie 1	30 October to 1 November	6.12	1.03	2.64
Vallocchie 2	30 October to 1 November	6.12	1.03	2.64
<b><i>M<sub>w</sub> 5.5 on 18 January 2017 10:14:19 (UTC)</i></b>				
S.Maria in Paganico	19 January	1.28	0.21	0.55

Note. Extrapolated peak ground velocities and the minimum/maximum range for the dynamic stress peak calculated at each mud volcano are reported.

<sup>a</sup>Exact time not determined.

Paganico MV, at Monteleone di Fermo, did not show any precursors (e.g., ground bulging) to eruption indicating an incipient activity associated with its cyclic nature and erupted with unexpected and strong flux. Another mud volcano, the Contrada S. Salvatore MV (newly formed at S. Vittoria in Matenano) located close to a farm, has been reported to erupt with an energetic flux, reaching up to 1.5–2 m high (as inferred from the mud deposited on the trees beside the mud volcano). The eruption of these mud volcanoes was immediately reported by local inhabitants familiar with these phenomena (e.g., at Monteleone di Fermo a natural reserve has been established around the mud volcanoes), and therefore, their occurrence after the earthquake cannot be coincidental. For comparison, only one eruption (at S. Maria in Paganico mud volcano, June 2016) was recorded in the 5 months before the onset of the seismic sequence in August 2016. If we extend our observation back in time, we can document one eruption in 2015 (Valle Corvone) and two eruptions in 2009 (S. Maria in Paganico and Valle Corvone). The number of eruptions has evidently increased after the 2016 seismic sequence.

We thus aim to test hypotheses for seismic triggering of these mud volcano eruptions, as documented in several studies (e.g., Chigira & Tanaka, 1997; Delisle, 2005; Martinelli et al., 1989; Rudolph & Manga, 2010; Rukavickova & Hanzl, 2008; Snead, 1964; Tsunogai et al., 2012). In particular, we investigate their activation after the major seismic events, specifically the  $M_w$  6.0 earthquake that hit the Amatrice-Accumoli area on 24 August 2016, the  $M_w$  6.5 Norcia event of 30 October 2016, and an  $M_w$  5.5 earthquake that hit the area of Montereale-Capitignano-Campotosto (Aquila Province) on 18 January 2017 (Figure 1a). We integrate field structural data collected on the mud volcanoes before (September 2015) and during the seismic sequence, with seismological data, to evaluate the correlation of triggered eruptions with peak ground velocity (PGV), dynamic stresses (peak dynamic stress), and static stresses (normal stress changes).

## 2. Geological Setting

The study area is part of the Marche Apennine foothills, where Mio-Pliocene marine sediments and Pleistocene continental deposits overly turbidite siliciclastic sediments that fill the Messinian foredeep basin (Bigi et al., 1999; Centamore et al., 1991). At the end of the Miocene-Early Pliocene, the area was then involved in the NE directed migration of the Apennine thrust-and-fold belt. In detail, the Messinian turbiditic deposits

belong to the Laga Formation, characterized by mainly pelitic and arenaceous lithofacies containing gypsum intercalations. The Laga Formation is overlain by the Colombacci Formation, which is composed of sandy-to-silty shales intercalated with calcareous levels. These deposits grade upward to the Pliocene sequence consisting of alternated marine mudstone-sandstone lithofacies belonging to the Argille Azzurre Formation. Quaternary continental deposits lie on top of the marine sequence, and outcrop in the Monteleone di Fermo area as a gently deformed NE dipping monocline.

The Argille Azzurre Formation is widely exposed around the Monteleone di Fermo area (Figure 1b) and continues in the subsurface down to a considerable depth, as shown by an available deep well (Figure 4c; the detailed stratigraphy of the wells in the area is available at the VIDEPI project website, <http://unmig.sviluppo-economico.gov.it/videpi/videpi.asp>). Mudstones are a favorable lithology for developing mud volcanoes because they provide an impermeable barrier that permits fluid overpressure to develop, and also furnish the solids entrained by the ascending aqueous fluids, generally a mixture of water and hydrocarbons in liquid and gaseous states (e.g., Kopf, 2002). The presence of fluids containing exsolved (or potentially exsolving) gases enables mud volcano formation, and once overpressures are sufficiently high, the upward migrating fluids have the ability to fluidize the mud and erupt it at surface.

### 3. Summary of the Central Italy Seismic Sequence and Mud Volcano Eruptions

The area affected by the 2016–2017 seismic sequence is a seismically active region that has been repeatedly struck by medium to large historical earthquakes produced by NW-SE trending normal faults (CPT115 catalogue; Rovida et al., 2016). The Amatrice sector was affected by four moderate to strong seismic events in 1627 ( $M_w$  5.3), 1639 ( $M_w$  6.2), 1646 ( $M_w$  5.9), and 1672 ( $M_w$  5.3) (CPT115 catalogue; Rovida et al., 2016). In more recent times, the  $M_w$  6.0 1997 Colfiorito seismic sequence hit northward, and the  $M_w$  6.3 2009 L'Aquila seismic sequence hit to the south of the study area (Figure 1a). The 2016–2017 earthquakes, struck an approximately 70 km long sector extending from Visso to L'Aquila, thus filling the seismic gap between the 1997 and 2009 seismic sequences (Figure 1a). The sequence, initiated with the  $M_w$  6.0 (or  $M_w$  6.1 depending on source; e.g., Tinti et al., 2016) Amatrice seismic event of 24 August 2016 (and not yet returned to the background rate of seismicity; Table 1), destroyed several historical small towns (i.e., Amatrice, Accumoli, Norcia, and Castelluccio di Norcia) and caused 299 casualties. Impressive coseismic effects were documented in the epicentral and surrounding areas (Livio et al., 2016; Pucci et al., 2017).

The  $M_w$  6.0 24 August 2016 earthquake was followed 1 h later by a  $M_w$  5.4 event, and 2 days later by two earthquakes, the largest of which had  $M_w$  5.9 and epicenter located near Visso (Figure 1a and Table 1). Immediately after (from a few hours, in the most favorable case, to maximum two days after) the  $M_w$  6.0 earthquake, three mud volcanoes erupted (Figure 2 and Table 2). The Santa Maria in Paganico mud volcano (referred hereafter to as S.M. in Paganico MV) and La Croce mud volcano erupted the day after the  $M_w$  6.0 earthquake, together with a third mud volcano here named Case Tedeschi 2Bis, located a few hundred meters south of La Croce mud volcano (Figures 2 and 3a, 3b, and 3e). The latter was dominated by a newly formed ground fracture emitting mud, located few meters from an older emission point (Figures 2 and 3e and Table 2). It is also noteworthy that eruptions of the S.M. in Paganico and La Croce mud volcanoes were also documented during the last decades. Before the 2016 seismic sequence the S.M. in Paganico MV registered large eruptions a couple of months after the  $M_w$  6.3 2009 L'Aquila earthquake and again in April and June 2016, with the latter activations speculatively also partly favored by the heavy rainfall that occurred during the previous days.

On 30 October 2016, the S.M. in Paganico and la Croce mud volcanoes erupted again after the  $M_w$  6.5 seismic event near Amatrice (Figures 1a and 2 and Tables 1 and 2). Other historically active mud volcanoes were also reactivated in the Monteleone di Fermo and adjoining areas (Figure 2 and Table 2): Case Tedeschi (different emission points were activated; Figure 2 and Table 2), Valle Corvone, and the Contrada S. Salvatore 1 (Figures 2 and 3c) (e.g., Ricci & Sciarra, 2016).

In addition, a few meters west of this emission point, at about 2:00 p.m. on 1 November 2016, a new mud volcano formed (here named Contrada S. Salvatore 2) and a new meter-scale open fracture emitted a watery fluid (referred to as Contrada S. Salvatore 3) (Figure 3d and Table 2, as documented by different media; Ricci & Sciarra, 2016). Three new emission points were also activated not far from the Monteleone di Fermo village (and therefore named Monteleone 1, 2, and 3 mud volcanoes; Figure 2 and Table 2).

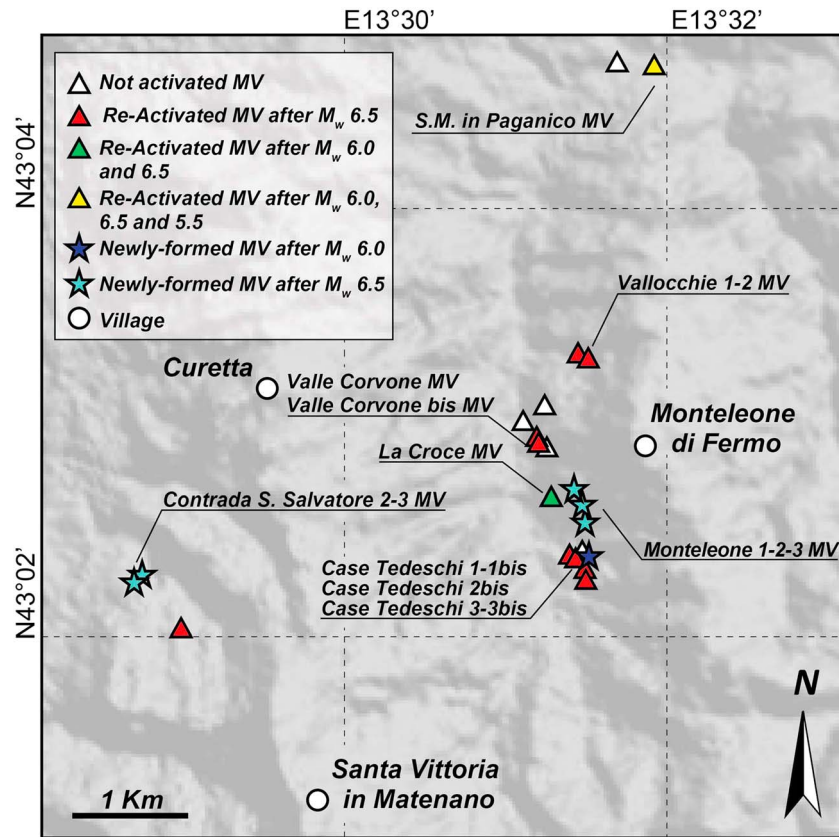


**Figure 2.** Location of the Monteleone di Fermo mud volcanoes. The different behavior shown by these features is reported.

Finally, the S.M. in Paganico MV increased its activity after the  $M_w$  5.1 and 5.5 seismic events of 18 January 2017 to the North of L'Aquila (Figure 1a and Tables 1 and 2). Two smaller earthquakes ( $M_w$  5.4 and 5.0) occurred in the same epicentral area after the major event (Table 1).

## 4. Methodology

### 4.1. Field and Seismic Data

Calculations of dynamic and static stresses require input parameters that in our case are produced by surface and subsurface geological data. In order to satisfy this requirement, we present the results of the survey that we carried out before (September 2015) and during the seismic sequence (October–November 2016), collecting structural data in the form of emission fracture orientations and mud volcano alignments and elongations (section 5.1). These data have been used as a proxy for the geometry of the subsurface feeder dyke system for the mud volcanoes, which is essential for calculating static stress changes (e.g., Bonini et al., 2016; section 4.3). Furthermore, we collected information from local inhabitants about the historical activity of mud volcanoes, their location, and past and no-longer visible features. Information about the subsurface geology necessary for estimating seismic velocities and dynamic stresses (see section 4.2) is obtained from literature data and the interpretation of three seismic reflection profiles (traces are indicated as AB, CD, and EF in Figures 1 and 4; see below section 5.1) provided by ENI S.p.A. The traces of profiles run close to the Monteleone di Fermo area, and a deep well available from the VIDEPI project (referred herein to as Well\_01) was used to correlate the seismic data to stratigraphy (Figures 1a and 4c).

### 4.2. Analysis of Dynamic Stress Changes

Passage of seismic waves generated by large earthquakes induces transient changes in stress at remote distances that can trigger local seismicity (Hill, 2008) and also enhance activity at volcanic systems (Avouris et al.,

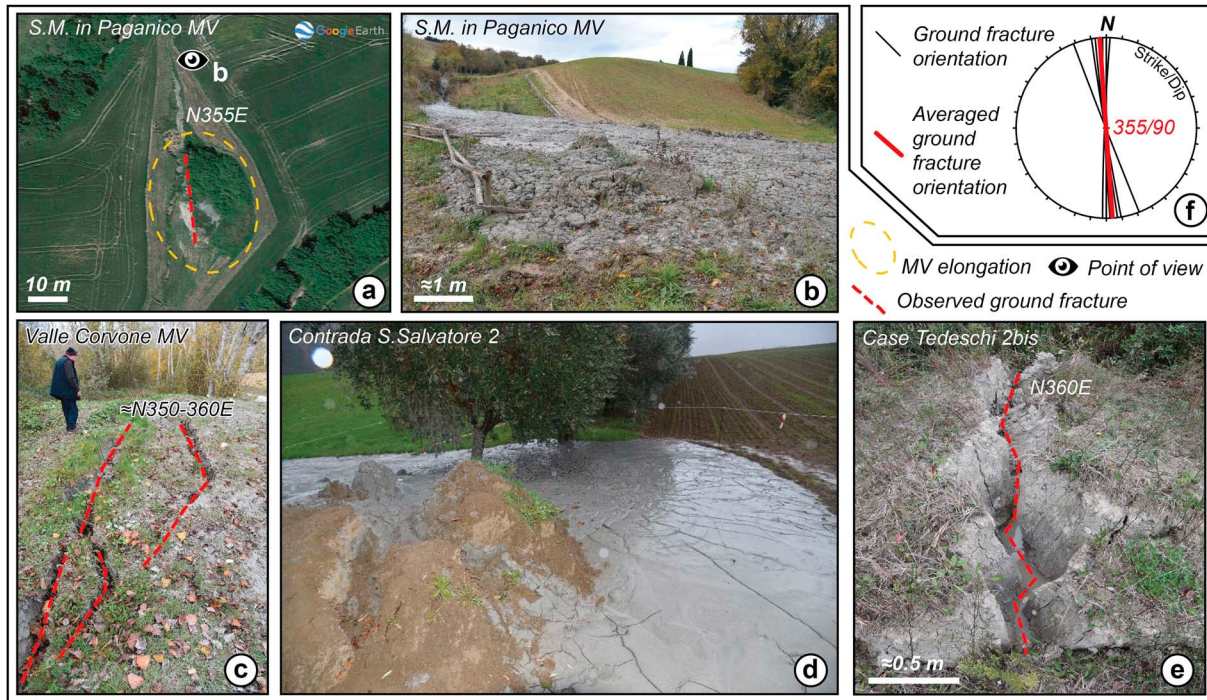


**Figure 3.** Examples of mud volcanoes that responded to the main earthquakes of the Central Italy seismic sequence. (a) Satellite image and (b) lateral view show the S.M. in Paganico mud volcano after the  $M_w$  6.5 earthquake of 30 October. (c) N-S trending fractures controlling the surface mud extrusion of the Valle Corvone mud volcano after the 30 October earthquake. (d) Lateral view of the newly formed Contrada S. Salvatore mud volcano, which erupted the day after the 30 October earthquake. (e) N-S trending fracture along the so-called Case Tedeschi 2bis mud volcano, a newly formed seep south of the Monteleone di Fermo village. (f) Stereoplot showing the trend of ground fractures controlling mud volcanism. An average value of  $N355^\circ \pm 5^\circ E/90^\circ$  is taken as input parameter for the normal stress change calculation.

2017; Delle Donne et al., 2010; Manga et al., 2012, 2009) by perturbing the dynamic equilibrium of crustal fluids (Hill, 2008).

To estimate the dynamic stress generated by the passing seismic waves, we use peak ground velocity (PGV) field from the Amatrice, Norcia, and Monteleone-Capitignano-Campotosto earthquakes, since peak ground velocity scales with the peak dynamic stress. We converted the earthquake peak ground velocities to stress using the following equation (Gomberg & Davis, 1996; Hill et al., 1993; Hong et al., 2016; Van Der Elst & Brodsky, 2010):

$$\sigma_r = \mu \frac{PGV}{\beta} \tag{1}$$

where  $\sigma_r$  is the radial peak dynamic stress, PGV is the peak ground velocities,  $\beta$  is the shear wave velocity, and  $\mu$  is the shear modulus. Shear modulus  $\mu$  can be derived from:

$$\mu = \rho \beta^2 \tag{2}$$

where  $\rho$  is the rock density. PGV for the Amatrice and Norcia seismic events are available in the ANSS Comprehensive Earthquake On-line Catalog (U.S. Geological Survey (USGS) shake map database; <https://earthquake.usgs.gov/earthquakes/eventpage/us10006g7d#shakemap>), which includes worldwide earthquake source parameters and other related products such as peak ground accelerations and velocities measured by contributing local seismic networks. We use the average PGV value among the three seismic components (vertical, north-south, and east-west) as the representative PGV value at the site. PGVs at mud volcanoes are then obtained by interpolating peak velocity measured by all seismic stations located within an area of  $\sim 36 \times 10^3 \text{ km}^2$ . PGV at the Earth surface is assumed to be comparable to the PGV experienced by the subsurface mud-fluid reservoir. The elastic parameters needed for calculating the peak dynamic stress are assumed to be in the range of the typical rock velocities (e.g., Bourbié et al., 1987), considering a host rock for the fluid-mud reservoir made of porous and saturated sandstones, such as those of the Laga Formation in

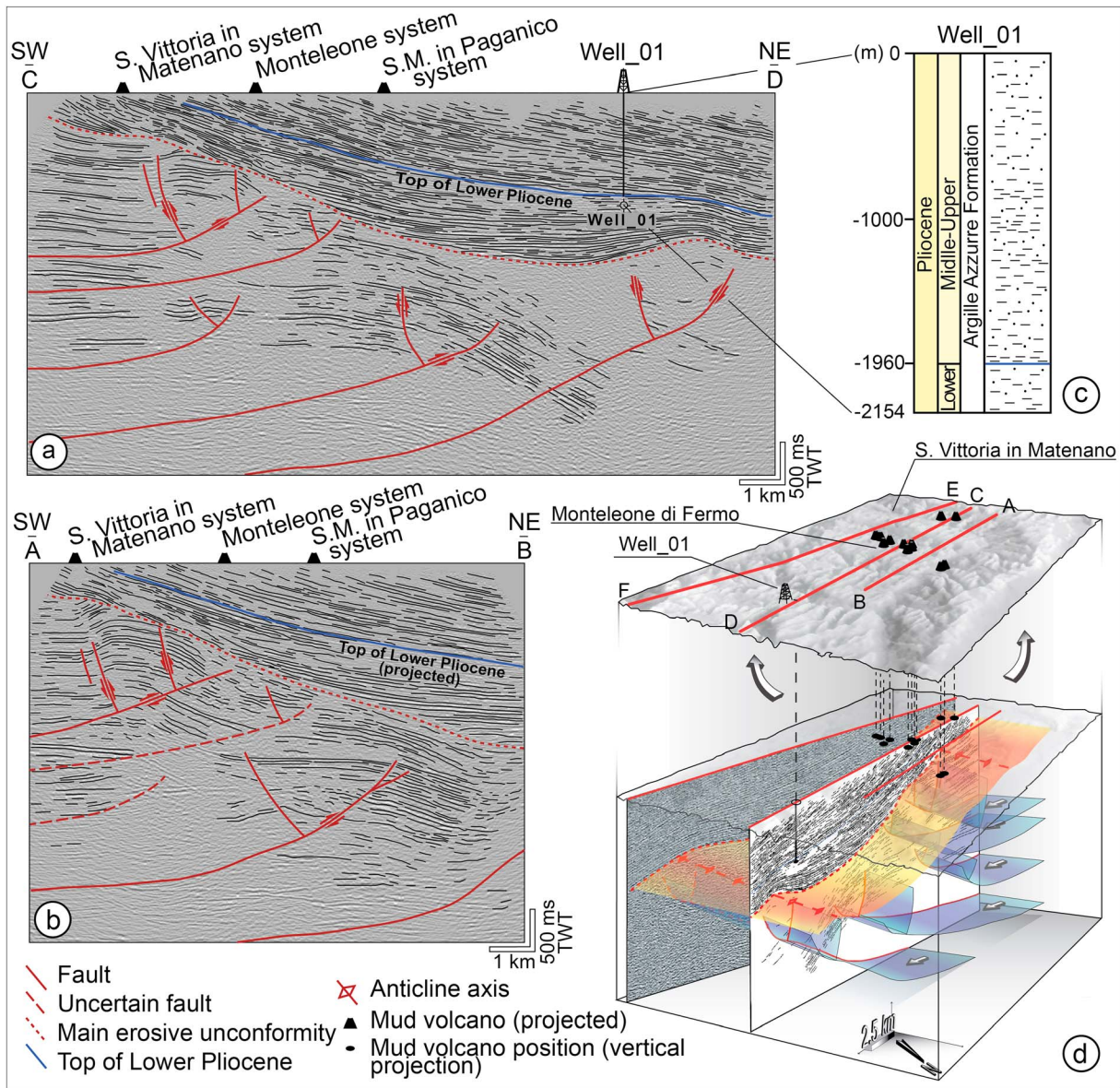


**Figure 4.** (a and b) Interpreted seismic sections used to constrain the subsurface setting of the mud volcanoes. (c) Schematic log of “well\_01.” This well and others in the adjoining areas are available at the VIDEPI project website <http://unmig.sviluppoeconomico.gov.it/videpi/videpi.asp>. (d) The 3-D block diagram showing the correspondence between the mud volcano systems and the underlying buried anticlines imaged in the seismic lines. Section EF (uninterpreted) is shown in the background.

the study area. Then, uncertainty in peak dynamic stress is related to uncertainties in rock density and shear wave velocities. On the basis of the regional geological framework, we estimate a minimum and a maximum bound for rock density (from 2,100 to 2,400 kg m<sup>-3</sup>) and for shear wave velocities (from 800 to 1,800 m/s) that are expected at a given mud volcano site. Doing so, we have calculated an expected range for peak dynamic stress, which allowed us to constrain a minimum and a maximum value. There is also uncertainty in the PGV used to compute the stress. We do not account for this (unknown) uncertainty in the reported stress uncertainty.

### 4.3. Analysis of Static Stress Changes

Static stress changes are permanent variations in the local stress field produced by slip on a fault (source fault). Stress changes decay with the epicentral distance ( $R$ ) as  $1/R^3$  and therefore become negligible a few fault lengths from the epicenter. Stress changes induced by an earthquake on a receiver fault or fracture

are given by the Coulomb Failure Function ( $\Delta CFF$ ) (e.g., King & Devès, 2015; King et al., 1994; Stein, 1999; Stein et al., 1992):

$$\Delta CFF = \Delta\tau + \mu(\Delta\sigma_n + \Delta P) \quad (3)$$

where  $\Delta\tau$  is the shear stress change on the receiver fault (direction of fault slip considered as positive),  $\Delta\sigma_n$  is the normal stress change (positive if the fault is unclamped),  $\mu$  is the friction coefficient, and  $\Delta P$  is the fault pore pressure change. Equation (3) is often simplified as

$$\Delta CFF = \Delta\tau + \mu' \Delta\sigma_n \quad (4)$$

where  $\mu'$  is the apparent coefficient of friction, which includes the effect of material properties and fluid pressure changes. In case of mud volcanoes, static stress changes (i.e., normal stress changes and volumetric changes) are thought to influence mud volcano activity when large enough and favorably oriented (Bonini et al., 2016). In particular, the normal stress change component ( $\Delta\sigma_n$ ) has been calculated in order to evaluate whether the stress variations act to close (clamp) or open (unclamp) the subsurface receiver feeder dyke system beneath the mud volcanoes.

The feeder dyke system is modeled as a vertical fracture representing an array of planar structures exploited by the ascending mud-fluid mixture. Accordingly, we did not compute shear stresses ( $\Delta\tau$ ) since they do not have a major effect on the opening (or closure) of fractures. Normal stress changes have been calculated in a homogeneous half-space (Okada, 1992) using the Coulomb software, version 3.3 (free download at <https://earthquake.usgs.gov/research/software/coulomb/>) (Toda et al., 2005, 2011). Since we had no quantitative information about material properties and heterogeneities, we assumed standard and homogeneous values. We have used the following values: Poisson's ratio ( $\nu$ ) = 0.25, Young's modulus ( $E$ ) =  $8 \times 10^5$  bar, shear modulus ( $G$ ) =  $3.2 \times 10^5$  bar, and apparent coefficient of friction ( $\mu'$ ) = 0.4 (e.g., King et al., 1994; Lin & Stein, 2004; Toda et al., 2005, 2011). Obviously, there might be uncertainties related to the use of these average values, but we do not have information to use more specific values.

## 5. Results

### 5.1. Surface and Subsurface Structural Controls on Mud Volcanoes

The geological survey revealed that mud discharge and eruption for many mud volcanoes are related to the formation of meter to tens of meter scale approximately N-S trending fractures, in some cases showing an echelon arrangement. Open fractures mainly strike between N350°E and 360°E and are characterized by an essentially vertical dip (Figure 3f). Elongation of the S.M. in Paganico MV is in agreement with this geometry (Figure 3a), as well as the alignment of minor emission points at the Valle Corvone MV (Figure 3c). Therefore, an average value of N355°E/90° has been considered as a reasonable approximation for the receiver feeder dyke system of mud volcanoes in the Monteleone di Fermo area and used for the calculation of the static stress changes.

No major structures controlling seepage have been identified during the fieldwork. Nonetheless, seismic lines imaged dominantly NE verging buried thrust anticlines and pop-up structures, which are overlain by an NE dipping monocline made up of marine Pliocene mudstones (Argille Azzurre Formation), as also confirmed by the available well that reaches a total depth of about 2,150 m (Figure 4). An unconformity marks the passage from the shallowest thrust folds to the monocline of Pliocene sediments (Figures 4a and 4b).

The imaged thrusts deform the lowest portion of the Pliocene sequence, suggesting a relatively recent influence of compressive deformation. The well (Figures 4a and 4c) does not reach the unconformity, yet it is likely that the sediments down to the base of the sequence consist of the same lithology, except probably immediately above the unconformity where the Colombacci Formation may be present. The anticlines' top is presumably composed of Miocene siliciclastic deposits of the Laga Formation, which are exposed in the western sector of the study area (Figure 1b). Interestingly, mud volcanoes dominantly localize over the hinge of the buried anticlines (Figures 4a, 4b, and 4d), as also documented in many other cases worldwide (e.g., Bonini, 2008; Jakubov et al., 1971). It is likely that the fluid reservoirs sourcing the mud volcanoes lie in the porous lithologies (Laga Formation) that occur at the core of the anticlines, below the impermeable Pliocene mudstones. Reservoir top varies between 1 and 2.5 km depending on the mud volcano, nonetheless, it is possible that shallower reservoirs in association with aquifers may be present in the porous members of the Pliocene sequence. The fluids ascend from anticlines and entrain mud, and eventually erupt when they are

transported up through pathways that reach the surface. Based on surface and subsurface information, the mud volcanoes in the Monteleone di Fermo area have been grouped into three systems, sourced by distinct reservoirs (Figure 1b). This approach has been extended to the other mud volcanoes of the Apennine foothills (see Figure 1a and Table S1 in the supporting information).

## 5.2. Peak Ground Velocity and Dynamic Stress Changes

Peak ground velocity (PGV) has been used in the past to find a link between ground motion and mud volcano response (Manga et al., 2009; Rudolph & Manga, 2012). In this study, PGVs of the three target seismic events are derived and interpolated from USGS and Istituto Nazionale di Geofisica e Vulcanologia (INGV) catalogues (<https://earthquake.usgs.gov/earthquakes/map/> and <http://cnt.rm.ingv.it/>). We have also estimated peak dynamic stresses following the attenuation relationship reported in section 4.2. The three PGV maps are shown in Figures 5a–5c, and the dynamic stress maps are reported in Figures 5d–5f. PGVs and maximum dynamic stresses have been then calculated from both types of maps at the position of each mud volcano.

The  $M_w$  6.0 Amatrice seismic event (Figure 5a) has PGV  $>14$  cm/s near the epicenter. At the three mud volcanoes that responded to this event, PGVs are 6.3 cm/s at the S.M. in Paganico MV and 7.3 cm/s at both La Croce and Case Tedeschi 2bis mud volcanoes (Table 2). Peak dynamic stress is in the range of  $\sim 1.1$ – $2.7$  bar at the S.M. in Paganico MV and  $\sim 1.3$  bar to  $\sim 3.2$  bar at both La Croce and Case Tedeschi 2bis mud volcanoes (Figure 5d and Table 2). Interestingly, both PGV and peak dynamic stress distribution maps show an elliptical protuberance elongated in a NE direction, which includes the Monteleone di Fermo mud volcanoes (Figures 5b and 5e). Larger PGV and stress values are calculated for the  $M_w$  6.5 Norcia earthquake of 30 October 2016. More than 10 mud volcanoes were activated after this event in the Monteleone di Fermo area (Table 2), with extrapolated PGV from 5.6 cm/s to 9.0 cm/s depending on the mud volcano location (Figure 5b and Table 2). The calculated peak transient dynamic stresses vary from  $\sim 0.9$ – $1.5$  bar (calculated using  $V_s = 800$  m/s) to  $\sim 2.4$ – $3.9$  bar (calculated using  $V_s = 1,800$  m/s) (Table 2). Notably, the contour lines define a NNE trending ellipse extending toward the area with the erupted mud volcanoes, thereby accounting for high PGVs and stress values (Figures 5b and 5e and Table 2). For the most recent  $M_w$  5.5 earthquake of 18 January 2017, only the S.M. in Paganico MV erupted. At the mud volcano position, PGV is  $\sim 1.3$  cm/s, and the peak dynamic stress is between  $\sim 0.2$  and 0.6 bar (Figures 5c and 5f and Table 2).

## 5.3. Static Stress Changes

We have calculated the normal stress changes at the erupted mud volcanoes for the three major seismic events (Table 1) and available source models (Tinti et al., 2016; Gruppo di Lavoro INGV sul terremoto in centro Italia, 2016). We used an average receiver feeder dyke trending  $N355^\circ E/90^\circ$  (see section 4.1). Uncertainties on this measured trend can be estimated as  $\pm 5^\circ$  (i.e., measurement error or local variation in the fracture trends). Such variation, tested in our models, substantially do not change outputs of dynamic stress change calculations. All the output results therefore refer to the  $N355^\circ \pm 5^\circ E/90^\circ$  trend. The input parameters of source model are described for each seismic event. We show here the results for some mud volcanoes that have shown remarkable postseismic activity (e.g., the S.M. in Paganico, La Croce, and Valle Corvone mud volcanoes) by responding shortly after (from few hours to a maximum of two days) with a strong mud-fluid flow, as well as those newly formed (e.g., Contrada S. Salvatore mud volcano), confirming that their activation was not coincidental.

### 5.3.1. The $M_w$ 6.0 (6.1) of 24 August 2016

The 24 August 2016 earthquake was modeled using the source model from Tinti et al. (2016) and the Aki and Richards (1980) convention. Tinti et al. (2016) calculate a  $M_w$  6.1 for this event and inverted strong motion data from the RAN (the Italian national accelerometric network) and INGV networks to estimate slip values on the fault plane. We modified Tinti et al. (2016) source fault in order to subdivide the calculated slip in 2.5 cm classes. The fault plane is oriented  $N156^\circ E$ ,  $50^\circ$  SW dipping, and is subdivided into 1,749 patches (constituting a  $16 \times 26$  km fault plane) to which a fixed slip value was assigned. Figure 6a shows the model. The three target mud volcanoes at Monteleone di Fermo are located close to the blue shadow, where normal stress changes are negative and therefore expected to clamp the feeder dyke. Negative normal stresses (at 0.5 km depth) are larger at the Valle Corvone mud volcano ( $-0.04$  bar), and less negative or close to zero at the S.M. in Paganico MV. Given the calculated values, normal stress changes cannot be considered influential on mud volcano eruptions.

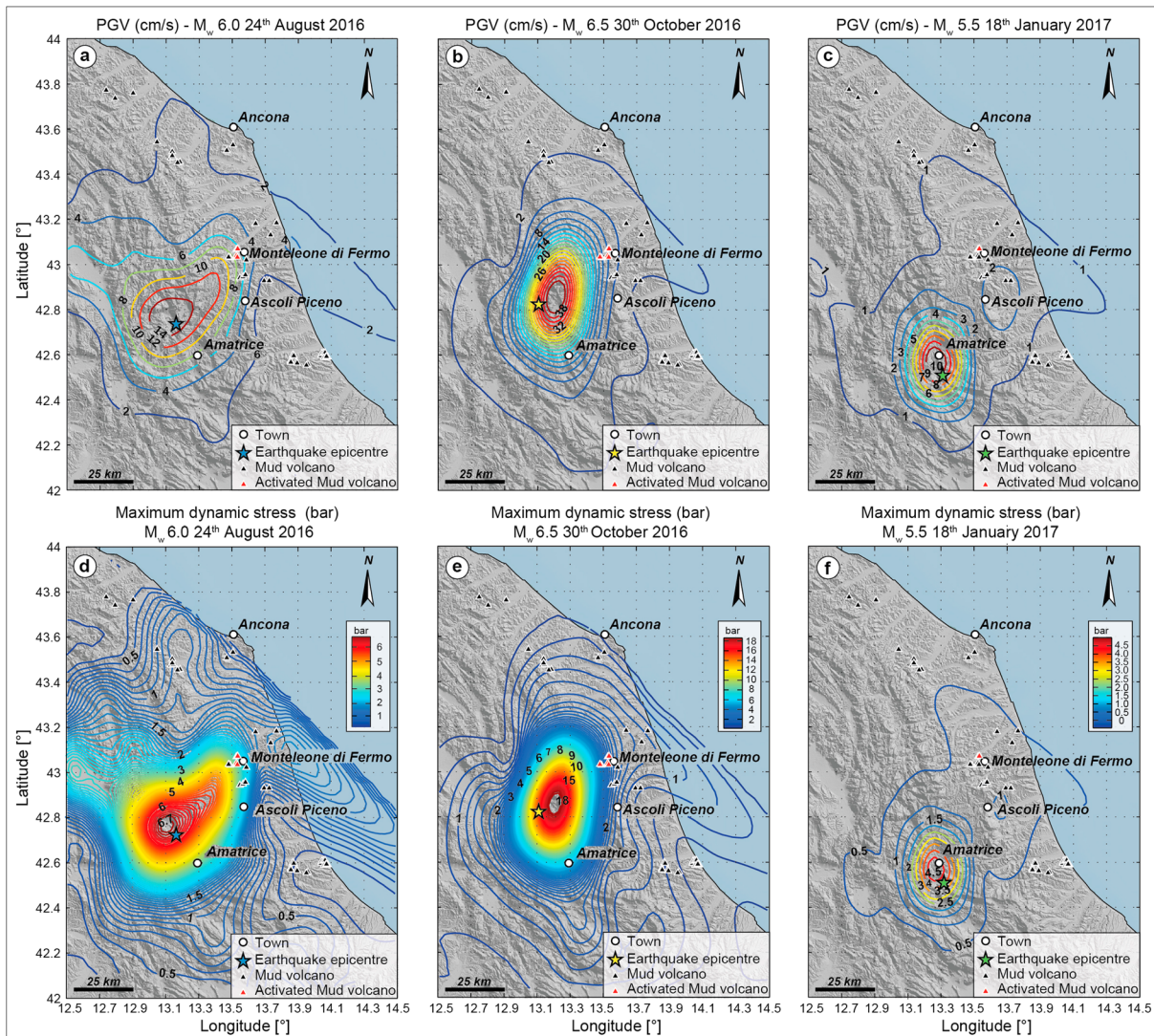


**Figure 5.** (a–c) Interpolated PGV maps for the three considered seismic events and (d–f) maps of maximum dynamic stress (see text for details). Isolines of warmer color indicate higher values, while cooler colors indicate lower values, both for PGVs and stresses. Note that the color bars in Figures 5d–5f do not have the same scale.

**5.3.2. The  $M_w$  6.5 of 30 October 2016**

The  $M_w$  6.5 30 October 2016 seismic event was modeled using the source model reported by Gruppo di Lavoro INGV sul terremoto in centro Italia (2016), with a N151°E and 47°SW dipping fault plane (30 × 16 km) subdivided into 120 patches. For slip vectors >40 cm, down-dip and right-lateral components were recalculated. Given the relatively high magnitude of the seismic event, the area affected by static stress changes has a radius of tens of kilometers (see Figure 6b). Nonetheless, the area with activated mud volcanoes completely falls in the negative clamping lobe (blue colors). Normal stress changes calculated at the mud volcanoes (0.5 km depth) are negative, varying from –0.44 bar at the Contrada S. Salvatore MV to –0.27 bar at the S.M. in Paganico MV. As in the case of the  $M_w$  6.0 Amatrice earthquake, normal stress changes are negative and therefore cannot have triggered the mud volcano eruption by unclamping a feeder dyke.

**5.3.3. The  $M_w$  5.5 of 18 January 2017**

Strong motion (or similar) source models were not available for the  $M_w$  5.5 earthquake of 18 January 2017. Therefore, we constrained the input parameters for the modeling using a focal mechanism solution (available at <http://cnt.rm.ingv.it/event/12697591>), with a fault plane oriented N161°E, dipping 50°SW, and rake of –86°. We implemented the source fault using a constant slip value by means of the empirical relation of Wells and

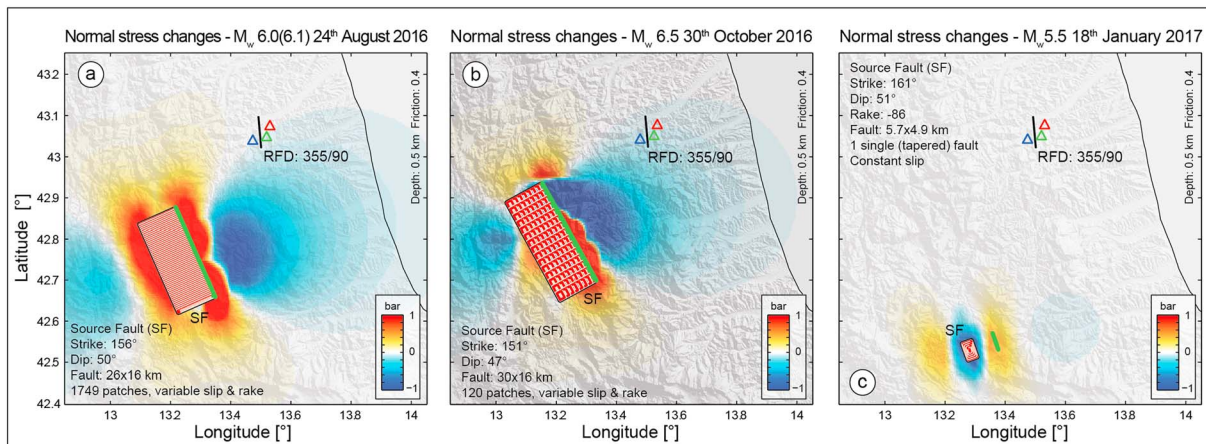


**Figure 6.** (a) Normal stress changes produced by the Amatrice earthquake, calculated using the source model with  $M_w$  6.1 proposed by Tinti et al. (2016). (b) Normal stress changes for the  $M_w$  6.5 Norcia seismic event. (c) Normal stress changes calculated for the  $M_w$  5.5 of 18 January 2017. SF, source fault; RFD, receiving feeder dyke. The triangles indicate the position of the mud volcano systems: blue, S. Vittoria in Matenano system; green, Monteleone system; red, S.M. in Paganico system.

Coppersmith (1994). Only the S.M. in Paganico MV was activated after this seismic event, where the calculated normal stress changes are extremely small (Figure 6c). In this last case, normal stress change probably had no effect on the mud volcanoes as their values were close to zero.

## 6. Discussion

Several mud volcanoes erupted in the Monteleone di Fermo area shortly after (hours to a maximum of 2 days) three major events (from  $M_w$  5.5 to  $M_w$  6.5) of the 2016–2017 seismic sequence in Central Italy (Table 2). Such a timing suggests a temporal correlation between the occurrence of the major earthquakes and the eruption of the mud volcanoes. We have therefore investigated separately the role of dynamic and static stress changes as possible eruption triggers. Before analyzing possible earthquake-induced stress triggers, we briefly discuss the potential role of local seismicity on paroxysmal activity of mud volcanoes. Several small-magnitude earthquakes ( $M_w \leq 3.0$ ) occurred in the Monteleone di Fermo area (INGV earthquakes catalogue, available at <http://cnt.rm.ingv.it>), but none of them immediately before mud volcano eruptions. The only exception is the  $M_w$  2.0 earthquake of 16 January 2017 that hit near S.M. in Paganico MV, but this event was too small and deep (hypocentral depth  $\sim 18$  km) to be influential. Therefore, a primary control of local seismicity on mud volcano eruptions can be ruled out. We also discard the possibility that groundwater changes due to rainfalls caused the 2016–2017 mud volcano eruptions. For instance, pluviometric data for the Monteleone di Fermo area (available online at Marche Region SIRMIP catalogue, website <http://84.38.48.145/sol/indexjs.php?lang=it>) record a cumulative rain fall of 0.6 mm and 47.8 mm during 10 days before the 24 August and 30 October earthquakes, respectively. Therefore, no heavy rain able to influence groundwater changes was registered, and a correlation with mud volcano triggering can be reasonably discarded. Furthermore, rainfall influences superficial reservoirs, while the main mud volcanoes reservoirs are here deeply rooted.

In order to evaluate the possibility of seismic triggering we plotted the relationship between earthquake magnitude and epicentral distance for both the present observations and other examples triggered mud eruptions (data compiled in Table S2 in the supporting information). Notably, all the Monteleone di Fermo mud volcanoes fall within distances for which other eruptions have been triggered (Figure 7). In addition, the obtained PGV values are similar to those reported for other cases of seismically triggered magmatic and mud volcanoes. The Niikappu mud volcano in Japan was triggered by earthquakes 6 times, with PGV between 8.3 and 107 cm/s (Manga et al., 2009; Table S2). Rudolph and Manga (2012) report PGV values in the range of 0.07–14.4 cm/s for the Davis-Schrimpf mud volcanoes, California, which showed responses to earthquakes during the period of April 2010 to February 2012. The PGV values for triggering define a wide range, and such an extreme variability may depend on whether it was a new eruption or the system was already erupting.

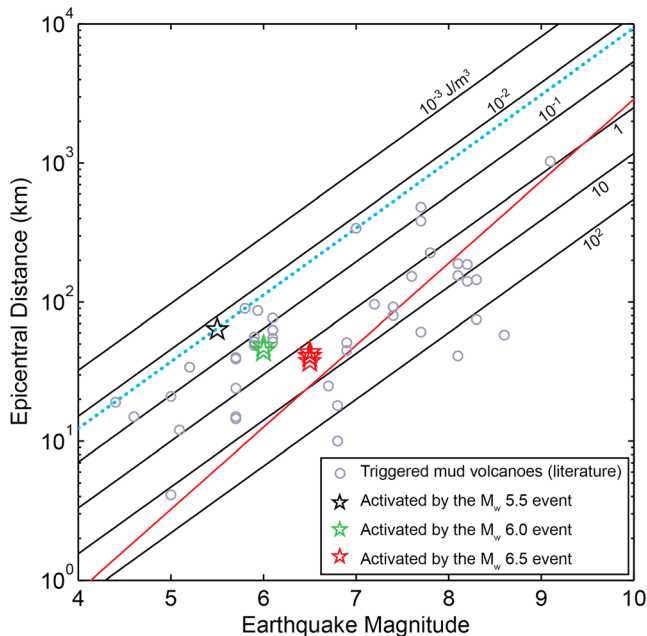


**Figure 7.** Magnitude versus epicentral distance graph showing literature data (grey circles; from Snead, 1964; Martinelli et al., 1989; Chigira & Tanaka, 1997; Delisle, 2005; Manga & Brodsky, 2006; Mellors et al., 2007; Bonini, 2009; Rukavickova & Hanzl, 2008; Manga et al., 2009; Rudolph & Manga, 2010; Rudolph & Manga, 2012; Tsunogai et al., 2012; Bonini et al., 2016. See also Table S2) for seismically triggered mud volcanoes. The stars indicate the new data for the Monteleone di Fermo mud volcanoes. The black lines are lines of constant seismic energy density using the empirical formulation in Wang and Manga (2010)—a measure of dynamic strain. The blue dotted line is the threshold energy for the most sensitive eruptions, and the red line is one fault length from the scaling in Wells and Coppersmith (1994).

mic events of Amatrice and Norcia. On the other hand, static stress changes might potentially influence the eruption by deforming the fluid/magma reservoir (e.g., Nostro et al., 1998). The plumbing of mud volcanoes is not well defined, particularly whether the fluid-mud mixture is contained in quasi-spherical chambers or in fissures/dykes, whose orientation at depth is unknown. Therefore, we are unable to evaluate static stress changes in fissure-shaped reservoirs. We could circumvent this problem by considering volumetric strain produced by the earthquakes on reservoirs. Taking the S. Maria in Paganico mud volcano as an example, both the  $M_w$  6.0 and  $M_w$  5.5 seismic events of 24 August 2017 and 18 January 2017 produced nil volumetric strain, while the  $M_w$  6.5 20 October 2016 event produced a volumetric contraction on the order of  $5 \times 10^{-7}$ , which would produce an increase in fluid pressure at the inferred reservoir depth. For a comparison, a volumetric strain on the order of  $10^{-6}$  is large enough to produce an increase in fluid pressure of 0.01 MPa (Roeloffs, 1996). Considering a linear relationship between volumetric strain and pore pressure variations (Roeloffs, 1996), the volumetric strain estimated at the mud volcano reservoir would be on the order of 0.005 MPa (0.05 bar), well below the “conventional” threshold of 0.1 bar. In all cases, the estimated magnitude of volumetric strain is small, and it thus likely not influential on the short-term response of the mud volcanoes. Peak dynamic stress is therefore the dominant, if not the only, candidate as a triggering mechanism for these eruptions.

In general, the mud volcanoes that responded to the main earthquakes ( $M_w$  6.0 and  $M_w$  6.5) experienced relatively large PGV and peak dynamic stress. However, peak dynamic stress calculated for the S.M. in Paganico MV eruption that followed the earthquake sequence of 18 January 2017 is lower, in the range of 0.21–0.55 bar (Table 2). Notably, only this system reacted to this seismic sequence, which consisted of four earthquakes ( $M_w$  5.0 to 5.5) that occurred in a very short time span (about 4 h; see Table 1). The response may reflect the cumulative effects of all earthquakes.

Furthermore, a comparison can be made with documented cases of seismic triggering of mud and magmatic volcanoes. Walter et al. (2007) report peak dynamic stresses between 0.1 and 0.6 bar at the Mount Merapi volcano, Indonesia, which was activated after two  $M_w$  6.3 seismic events (the first in 2001 and the second in 2006, both with epicenters about 50 km from the volcano). A comparison between mud volcanoes and magmatic volcanoes may be not straightforward, but it can be proposed on the basis of the similarities (e.g., eruptive history, internal structure, and buoyancy driven by exsolved gas; Stewart & Davies, 2006; Evans et al., 2008; Kopf, 2008; Manga et al., 2009) between these apparently distinct processes. In addition, Wang and Manga (2010) propose that the seismic energy density threshold for triggering, as well as the epicentral distance for triggering, is the same for both magmatic and mud volcanoes.

Extrapolated PGVs at mud volcanoes that were activated shortly (hours to a maximum of 2 days; Table 2) after the 24 August and 30 October 2016 earthquakes vary from ~5.6 to 9 cm/s, and the calculated peak dynamic stresses vary in the range between 0.94 bar and 3.89 bar (see section 5.2; Table 2). These values often exceed or are comparable to the stress magnitude reported for other triggered events such as changes in the water level in wells, triggered earthquakes, and changes in the behavior of geysers (e.g., Manga et al., 2009; Rudolph & Manga, 2012).

In addition, the static normal stress changes calculated at the erupted mud volcanoes are negative and/or negligible (section 5.3). This suggests that static stresses have either acted to close the feeder dykes (thereby discouraging mud eruption) or were too small to have an influence (Stein, 1999, suggests 0.1 bar as seismic triggering threshold). On this basis, static stresses did not influence appreciably the mud volcano eruptions that occurred shortly after the  $M_w$  6.0 and  $M_w$  6.5 seismic events of Amatrice and Norcia.

The Monteleone di Fermo area experienced relatively high PGV and peak dynamic stress values (Figure 5). In particular, contour lines of PGV and dynamic stress elongate suborthogonal to the source fault strike. At a first glance, this feature might be associated with fault rupture directivity. Kilb et al. (2000, 2002) show that directivity effects are related to rupture propagation that in turn influences the asymmetric distribution of dynamic stresses, while the pattern of static stresses is essentially unrelated to directivity. Given that dynamic stress directivity occurs along the rupture strike, rupture directivity effects might not be the best candidate to explain the PGV distribution pattern. The latter is related to the radiation pattern of the seismic waves. Surface Rayleigh and Love waves (e.g., Stein & Wysession, 2003) and *S* waves (e.g., Bormann et al., 2012) show a radiation pattern that is generally orthogonal to the fault strike, a characteristic that is common to the observed PGV distribution (Figures 5a–5c). Seismic shaking is primarily associated with the passage of *S* waves; therefore, we propose that PGV asymmetry might be mostly associated with the *S* waves radiation pattern. The occurrence of relatively high-magnitude PGV values might explain why only mud volcanoes in the Monteleone di Fermo area were triggered out of all the others in the region (see Figure 1a) but still does not explain why not all of those in the Monteleone di Fermo area were triggered.

A key outstanding question is why in the case of the 18 January 2017 earthquake ( $M_w$  5.5) only the S.M. in Paganico MV erupted. We suggest that this behavior is consistent with the idea that some erupting systems require less stress to be activated (e.g., Bonini et al., 2016). On the other hand, other mud volcanoes were in similar conditions but did not react. One possibility is that the S.M. in Paganico MV was near a critical state, and thus on the verge of erupting, independent of any earthquakes, consistent with the observation that this system also erupted a few months before (i.e., April and June 2016) the 24 August earthquake. If this is the case, even a small dynamic stress may be sufficient to trigger an eruption. A number of mud volcanoes did not erupt even though they experienced PGV and peak dynamic stress of the same order of those that erupted. We illustrate this behavior by plotting, for each main earthquake, the epicentral distance versus the peak dynamic stress calculated at mud volcano systems (Figures 8a–8c). It is important to note that for this analysis we considered systems of mud volcanoes, i.e., groups of emitting points or seeps fed from distinct subsurface reservoirs. This choice is based on the assumption that the eruption (or the paroxysmal activity) of even a few out all the seeps of a system identifies the system as being triggered. The inactivity of single seeps may depend on local causes (e.g., conduit sealing, opening, and abandoning of fluid pathways, activity at other seeps). Nevertheless, we also note that some mud volcano systems experiencing high strain were not activated, a circumstance that is particularly evident for the earthquake of 24 August 2016 (Figure 8a). The reasons of such behavior are unknown but may reflect the state of the mud volcano state prior to the earthquake (such as internal pressure and conduit healing).

Furthermore, this probably indicates that the link between the passing seismic waves and triggering mud volcano eruptions is not trivial. It is likely that duration of the shaking associated with the seismic event in addition to the amplitude/frequency of the seismic waves may play a role. For example, experimental data (Popescu, 2002; Popescu et al., 2006) and field data (Manga et al., 2009; Rudolph & Manga, 2012) show that for a given amplitude, low frequencies are more effective in increasing pore pressures, dislodging bubbles and particle of the fluid/mud matrix, and therefore increasing fluid mobility and discharge. Mellors et al. (2007) and Rudolph and Manga (2012) suggest that also the duration of the shaking can influence the liquefaction processes, enhancing the possibility of dynamic triggering of mud volcanoes.

One could also raise the question about the time delay (hours to days) between the earthquakes and the eruptions. Such a short delay is probably linked to the eruption mechanism—it takes a finite time for mud and fluids to ascend from the source region. Several triggering mechanisms have been proposed in the literature (e.g., Manga et al., 2009), and links have been made to several attributes of the earthquake such as frequency and duration and amplitude. A further mechanism potentially driving the eruption is the so-called “advective overpressure,” which takes into account the time required for the bubbles at the bottom of the reservoir (that experience a higher pressure compared to bubbles at the top) to reach the reservoir top. This time might explain the observed short time delay. Nonetheless, this process is not expected to be frequency or time-dependent (Manga et al., 2009), and it is not expected to be the only and principal eruption mechanism, due to unlikely gas oversaturation of the mud-fluid mixture, and its compressibility. Given that the mud volcanoes are in far-field, it is unlikely that postseismic effects will be relevant for mud volcanoes unless they break barriers to fluid transport. These types of postseismic effects are analogous to static strains, and they are small in magnitude.

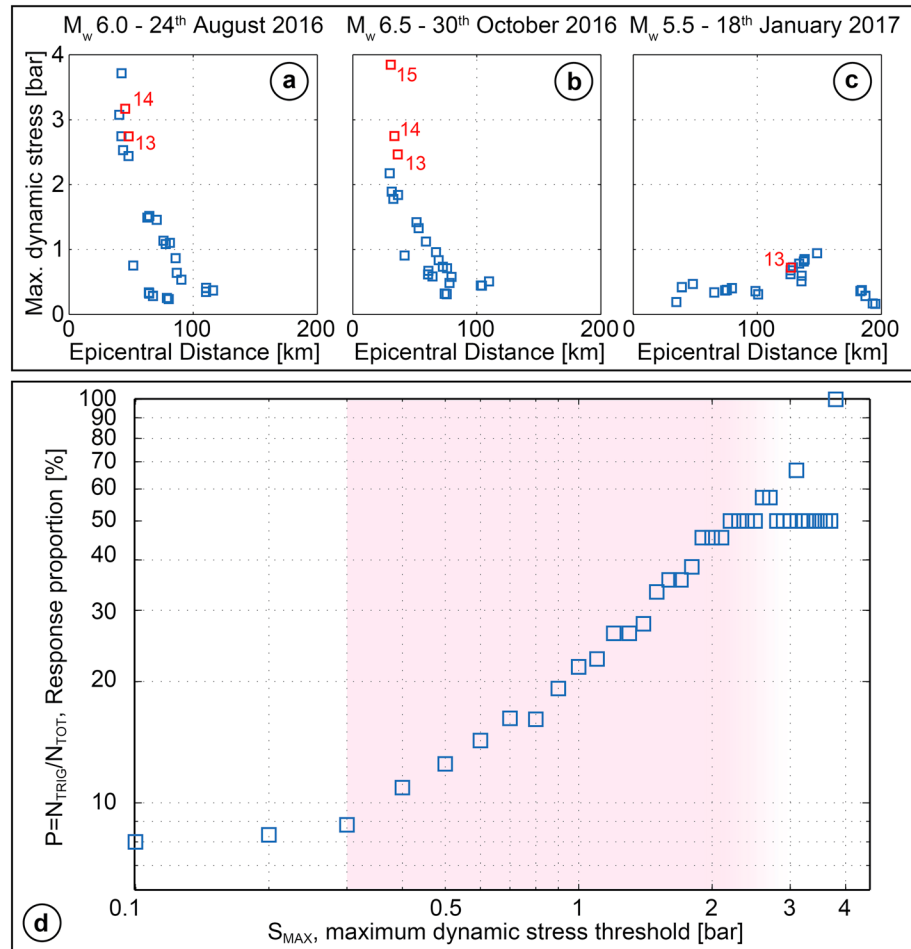


**Figure 8.** (a–c) Epicentral distance versus peak dynamic stress at mud volcano systems for the three considered seismic events. The red squares indicate triggered mud volcano systems (the red number beside the square refers to Table S1). (d) Response proportion  $P$  as a function of the ratio between the number of mud volcano systems showing onset of activity after an earthquake ( $N_{TRIG}$ ), and the total number of mud volcano systems ( $N_{TOT}$ ), which were affected by a peak dynamic stress greater than an incrementally increased threshold. A positive correlation between the response proportion and peak dynamic stress threshold demonstrates the linkage between earthquake shaking and mud volcanic activity.

Finally, observations of triggered eruptions provide a basis for attempting to constrain the relationship between earthquake shaking and mud volcano response. We define the response proportion in terms of a cumulative response ratio,  $P (>S_{MAX})$ , which considers the ratio between the number of positive responses (i.e., onset of mud volcanic activity after earthquake occurrence),  $N_{TRIG} (\geq S_{MAX})$ , and the total number of mud volcanic systems  $N_{TOT} (\geq S_{MAX})$  that have been affected by a peak dynamic stress greater than  $S_{MAX}$  (with  $S_{MAX}$  being an incrementally increased threshold) (Figure 8d). We find that the response ratio increases exponentially with peak dynamic stress. As a result, the response ratio increases from  $<10\%$  for peak dynamic stress  $>0.3$  bar to  $>50\%$  for peak dynamic stress  $>2$  bar, thus demonstrating a close link between earthquake shaking and onset of mud volcanic activity (Figure 8d).

### 7. Conclusions

We have shown that there is a temporal correlation between the major seismic events of the 2016–2017 seismic sequence of Central Italy and the eruption of some of the Montelone di Fermo mud volcanoes. Seismic triggering is suggested by the relatively short delay time between the eruptions and the earthquakes, which spans from few hours to a maximum of 2 days, as well as by the large number of eruptions (at least 20) that occurred during the seismic sequence in comparison to the single eruption in the 5 months before the seismic sequence onset. In order to assess the role of earthquake-generated stresses on mud volcano triggering,

we have evaluated peak dynamic stresses and static stress changes for three major seismic events, namely, the Amatrice earthquake ( $M_w$  6.0) of 24 August 2016, the Norcia earthquake ( $M_w$  6.5) of 30 October 2016, and the main seismic event ( $M_w$  5.5) of the Monteleone-Capitignano-Campotosto sequence of 18 January 2017. Static normal stress changes are either negative or exceedingly small, the calculated values ranging between  $-0.44$  and  $0$  bar. Hence, they are not likely to have influenced mud volcano activity by clamping the feeder dyke systems. Peak transient dynamic stresses, however, were much. In particular, the calculated maximum dynamic stresses at the locations of the mud volcanoes reach values up to  $3.9$  bar. For this reason, peak dynamic stresses are inferred to be the dominant driver triggering the several mud eruptions that followed the main seismic shocks of 24 August and 30 October 2016. The number of triggered mud volcanoes is likely related to the shaking registered at the mud volcano position. The calculated response ratio, the fraction of activated mud volcanoes above a certain peak dynamic stress values, increases from  $<10\%$  for dynamic stress  $>0.3$  bar to  $>50\%$  for dynamic stress  $>2$  bar.

### Acknowledgments

We acknowledge Deborah Kilb and an anonymous reviewer for their constructive and insightful comments that improved the manuscript. We kindly thank ENI S.p.A. and Alessandro Fattorini for providing us the seismic sections and allowing us to show them in this article. We also thank the Municipality of Monteleone di Fermo and in particular the Major Marco Fabiani and Stefano Pagliuca for assistance during the survey. We gratefully acknowledge the Osservatorio Geologico di Coldigioco (OGC) and its director, Alessandro Montanari, for providing us information on some of the Marche mud volcanoes and for hosting us at OGC. Used well and others are available at the VIDEPI Project website (<http://unmig.sviluppo-economico.gov.it/videpi/videpi.asp>). PGVs are available at the USGS Earthquake Hazard Program website (<https://earthquake.usgs.gov/earthquakes/>), and focal mechanisms are available at the INGV website (<http://cnt.rm.ingv.it/>). Pluviometric data from SIRMIP catalogue are accessible at <http://84.38.48.145/sol/indexjs.php?lang=itare>. This work was supported by Tuscan Earth Science PhD Program (Regional Grant Pegaso) [grant POR ICO FSE 2014/2020-Asse C], the National Research Council of Italy (CNR)-Regione Toscana [grant 0003084], U.S. National Science Foundation [grant NSF EAR1344424], and the University of Florence [ordinary funds 2014–2015].

### References

- Aki, K., & Richards, P. G. (1980). *Quantitative seismology* (p. 932). New York: W.H. Freeman & Co.
- Avouris, D. M., Carn, S. A., & Waite, G. P. (2017). Triggering of volcanic degassing by large earthquakes. *Geology*, *45*(8). <https://doi.org/10.1130/G39074.1>
- Bigi, S., Calamita, F., Cello, G., Centamore, E., Deiana, G., Paltrinieri, W., & Ridolfi, M. (1999). Tectonics and sedimentation within a Messinian foredeep in the Central Apennines, Italy. *Journal of Petroleum Geology*, *22*(1), 5–18. <https://doi.org/10.1111/j.1747-5457.1999.tb00456.x>
- Bonaserà, F. (1952). I vulcanelli di Fango del Preappennino Marchigiano. *Rivista Geografica Italiana*, *59*, 16–26.
- Bonaserà, F. (1954). I vulcanelli di Fango dell'Abruzzo orientale. *Rivista Geografica Italiana*, *61*, 217–223.
- Bonini, M. (2008). Elliptical mud volcano caldera as stress indicator in an active compressional setting (Nirano, Pede-Apennine margin, northern Italy). *Geology*, *36*(2), 131–134. <https://doi.org/10.1130/G24158A.1>
- Bonini, M. (2009). Mud volcano eruptions and earthquakes in the Northern Apennines and Sicily, Italy. *Tectonophysics*, *474*(3), 723–735. <https://doi.org/10.1016/j.tecto.2009.05.018>
- Bonini, M., Rudolph, M. L., & Manga, M. (2016). Long- and short-term triggering and modulation of mud volcano eruptions by earthquakes. *Tectonophysics*, *672–673*, 190–211. <https://doi.org/10.1016/j.tecto.2016.01.037>
- Bormann, P., Wendt, S., & Starke, U. (2012). Radiation patterns of earthquake fault mechanisms. In P. Bormann (Ed.), *New Manual of seismological observatory practice, Information Sheet 1.1* (pp. 12–18). Potsdam, Germany: GeoForschungsZentrum.
- Bourbié, T., Coussy, O., & Zinszner, B. (1987). *Acoustics of Porous Media*, (Editions Technip ed., p. 334). France: Saint-Jean-de-Braye.
- Capozzi, R., & Picotti, V. (2002). Fluid migration and origin of a mud volcano in the Northern Apennines (Italy): The role of deeply rooted normal faults. *Terra Nova*, *14*(5), 363–370. <https://doi.org/10.1046/j.1365-3121.2002.00430.x>
- Capozzi, R., & Picotti, V. (2010). Spontaneous fluid emissions in the Northern Apennines: geochemistry, structures and implications for the petroleum system. *Geological Society, London, Special Publications*, *348*(1), 115–135. <https://doi.org/10.1144/SP348.7>
- Centamore, E., Cantalamessa, G., Micarelli, A., Potetti, M., Berti, D., Bigi, S., ... Ridolfi, M. (1991). Stratigrafia e analisi di facies dei depositi del Miocene e del Pliocene inferiore dell'avanfossa marchigiano-abruzzese e delle zone limitrofe. *Studi Geologici Camerti*, *2*, 125–131.
- Cheloni, D., De Novellis, V., Albano, M., Antonioli, A., Anzidei, M., Atzori, S., ... Doglioni, C. (2017). Geodetic model of the 2016 Central Italy earthquake sequence inferred from InSAR and GPS data. *Geophysical Research Letters*, *44*, 6778–6787. <https://doi.org/10.1002/2017GL073580>
- ChiaraLuca, L., Di Stefano, R., Tinti, E., Scognamiglio, L., Michele, M., Casarotti, E., & Lombardi, A. (2017). The 2016 Central Italy seismic sequence: A first look at the mainshocks, aftershocks, and source models. *Seismological Research Letters*, *88*(3), 757–771. <https://doi.org/10.1785/0220160221>
- Chigira, M., & Tanaka, T. (1997). Structural features and the history of mud volcanoes in southern Hokkaido, northern Japan. *Journal of Geological Society of Japan*, *103*, 781–791. <https://doi.org/10.5575/geosoc.103.781>
- Damiani, A. V. (1964). Studio della salsa di Offida (Ascoli Piceno-Marche). *L'Universo*, *3*, 473–487.
- Delisle, G. (2005). Mud volcanoes of Pakistan—An overview. In G. Martinelli & B. Panahi (Eds.), *Mud volcanoes, geodynamics and seismicity, NATO Science Series, Earth and Environmental Sciences* (Vol. 51, pp. 159–169). Dordrecht, Netherlands: Springer. [https://doi.org/10.1007/1-4020-3204-8\\_14](https://doi.org/10.1007/1-4020-3204-8_14)
- Delle Donne, D., Harris, A. J. L., Ripepe, M., & Wright, R. (2010). Earthquake-induced thermal anomalies at active volcanoes. *Geology*, *38*(9), 771–774. <https://doi.org/10.1130/G30984.1>
- Evans, R. J., Stewart, S. A., & Davies, R. J. (2008). The structure and formation of mud volcano summit calderas. *Journal of the Geological Society of London*, *165*, 769–780. <https://doi.org/10.1144/0016-76492007-118>
- Gomberg, J., & Davis, S. (1996). Stress/strain changes and triggered seismicity at The Geysers, California. *Journal of Geophysical Research*, *101*(B1), 733–749. <https://doi.org/10.1029/95JB03250>
- Gruppo di Lavoro INGV sul terremoto in centro Italia (2016). *Rapporto di sintesi sul Terremoto in centro Italia  $M_w$  6.5 del 30 ottobre 2016*; <https://doi.org/10.5281/zenodo.166019>
- Hill, D. P. (2008). Dynamic stresses, Coulomb failure, and remote triggering. *Bulletin of the Seismological Society of America*, *98*(1), 66–92. <https://doi.org/10.1785/0120070049>
- Hill, D. P., Reasenberg, P. A., Michael, A., Arabaz, W. J., Beroza, G., Brumbaugh, D., ... Zollweg, J. (1993). Remote seismicity triggered by the  $M7.5$  Landers, California earthquake of June 28, 1992. *Science*, *260*, 1617–1623. <https://doi.org/10.1126/science.260.5114.1617>
- Hong, T.-K., Choi, E., Park, S., & Shin, J. S. (2016). Prediction of ground motion and dynamic stress change in Baekdusan (Changbaishan) volcano caused by a North Korean nuclear explosion. *Scientific Reports*, *6*(October 2015), 21477. <https://doi.org/10.1038/srep21477>
- Jakubov, A. A., Ali-Zade, A. A., & Zeinalov, M. M. (1971). *Mud Volcanoes of the Azerbaijan SSR*. Baku: Atlas (in Russian), Azerbaijan Academy of Sciences.
- Kilb, D., Gomberg, J., & Bodin, P. (2000). Triggering of earthquake aftershocks by dynamic stress. *Nature*, *408*(6812), 570. <https://doi.org/10.1038/35046046>

- Kilb, D., Gomberg, J., & Bodin, P. (2002). Aftershock triggering by complete Coulomb stress changes. *Journal of Geophysical Research*, *107*, 2060. <https://doi.org/10.1029/2001JB000202>
- King, G. C. P., & Devès, M. H. (2015). Fault interaction, earthquake stress changes, and the evolution of seismicity. *Treatise on Geophysics. Earthquake Seismology*, Chapter 10, 4, 225–255. <https://doi.org/10.1016/B978-0-444-53802-4.00077-4>
- King, G. C. P., Stein, R. S., & Lin, J. (1994). Static stress changes and the triggering of earthquakes. *Bulletin of the Seismological Society of America*, *84*, 935–953.
- Kopf, A. J. (2002). Significance of mud volcanism. *Reviews of Geophysics*, *40*, 1005. <https://doi.org/10.1029/2000RG000093>
- Kopf, A. J. (2008). Making calderas from mud. *Nature Geoscience*, *1*, 500–501. <https://doi.org/10.1038/ngeo256>
- Lin, J., & Stein, R. (2004). Stress triggering in thrust and subduction earthquakes, and stress interaction between the southern San Andreas and nearby thrust and strike-slip faults. *Journal of Geophysical Research*, *109*, B02303. <https://doi.org/10.1029/2003JB002607>
- Livio, F., Michetti, A. M., Vittori, E., Gregory, L., Wedmore, L., Piccardi, L., ... Central Italy Earthquake Working Group (2016). Surface faulting during the August 24, 2016, central Italy earthquake ( $M_w$  6.0): preliminary results. *Annals of Geophysics*, *59*, 1–8. <https://doi.org/10.4401/ag-7197>
- Lupi, M., Ricci, B. S., Kenkel, J., Ricci, T., Fuchs, F., Miller, S. A., & Kemna, A. (2015). Subsurface fluid distribution and possible seismic precursory signal at the Salse di Nirano mud volcanic field, Italy. *Geophysical Journal International*, *204*, 907–917. <https://doi.org/10.1093/gji/ggv454>
- Manga, M., & Bonini, M. (2012). Large historical eruptions at subaerial mud volcanoes, Italy. *Natural Hazards and Earth System Sciences*, *12*(11), 3377. <https://doi.org/10.5194/nhess-12-3377-2012>
- Manga, M., & Brodsky, E. E. (2006). Seismic triggering of eruptions in the far field: Volcanoes and geysers. *Annual Review of Earth and Planetary Sciences*, *34*, 263–291. <https://doi.org/10.1146/annurev.earth.34.031405.125125>
- Manga, M., Brumm, M., & Rudolph, M. L. (2009). Earthquake triggering of mud volcanoes. *Marine and Petroleum Geology*, *26*(9), 1785–1798. <https://doi.org/10.1016/j.marpetgeo.2009.01.019>
- Manga, M., Beresnev, I., Brodsky, E. E., Elkhoury, J. E., Elsworth, D., Ingebritsen, S. E., & Wang, C. Y. (2012). Changes in permeability caused by transient stresses: Field observations, experiments, and mechanisms. *Reviews of Geophysics*, *50*, RG2004. <https://doi.org/10.1029/2011RG000382>
- Martinelli, G., & Judd, A. (2004). Mud volcanoes of Italy. *Geological Journal*, *39*(1), 49–61. <https://doi.org/10.1002/gj.943>
- Martinelli, G., Bassignani, A., Ferrari, G., & Finazzi, P. B. (1989). Predicting earthquakes in Northern Apennines: Recent developments in monitoring of Radon 222. *Proceedings of the 4th International Symposium on The Analysis of Seismicity and Seismic Risk*, Bechyne Castle, Czechoslovakia, 4–9 September 1989 (pp. 192–208).
- Mellors, R., Kilb, D., Aliyev, A., Gasanov, A., & Yetirmishli, G. (2007). Correlations between earthquakes and large mud volcano eruptions. *Journal of Geophysical Research*, *112*, B04304. <https://doi.org/10.1029/2006JB004489>
- Nostro, C., Stein, R. S., Cocco, M., Belardinelli, M. E., & Marzocchi, W. (1998). Two-way coupling between Vesuvius eruptions and Southern Apennine earthquakes, Italy, by elastic stress transfer. *Journal of Geophysical Research*, *103*, 24,487–24,504. <https://doi.org/10.1029/98JB00902>
- Okada, Y. (1992). Internal deformation due to shear and tensile faults in a half-space. *Bulletin of the Seismological Society of America*, *82*(2), 1018–1040.
- Oppo, D., Capozzi, R., & Picotti, V. (2013). A new model of the petroleum system in the Northern Apennines, Italy. *Marine and Petroleum Geology*, *48*, 57–76. <https://doi.org/10.1016/j.marpetgeo.2013.06.005>
- Planke, S., Svensen, H., Hovland, M., Banks, D. A., & Jamtveit, B. (2003). Mud and fluid migration in active mud volcanoes in Azerbaijan. *Geo-Marine Letters*, *23*, 258–268. <https://doi.org/10.1007/s00367-003-0152-z>
- Popescu, R. (2002). Finite element assessment of the effects of seismic loading rate on soil liquefaction. *Canadian Geotechnical Journal*, *39*(2), 331–344.
- Popescu, R., Prevost, J. H., Deodatis, G., & Chakraborty, P. (2006). Dynamics of nonlinear porous media with applications to soil liquefaction. *Soil Dynamics and Earthquake Engineering*, *26*(6-7), 648–665.
- Pucci, S., De Martini, P. M., Civico, R., Villani, F., Nappi, R., Ricci, T., ... Pantosti, D. (2017). Coseismic ruptures of the 24 August 2016,  $M_w$  6.0 Amatrice earthquake (central Italy). *Geophysical Research Letters*, *44*, 2138–2147. <https://doi.org/10.1002/2016GL071859>
- Ricci, T., & Sciarra, A. (2016). Sequenza sismica in Italia centrale: I vulcanelli di fango in provincia di Fermo. Report Gruppo operativo EMERGEO, INGV. Retrieved from <https://ingvterremoti.wordpress.com/2016/11/11/sequenza-sismica-in-italia-centrale-i-vulcanelli-di-fango-in-provincia-di-fermo/>
- Roeloffs, E. (1996). Poroelastic techniques in the study of earthquake-related hydrologic phenomena. *Advances in Geophysics*, *37*, 135–195.
- Rovida, A., Locati, M., Camassi, R., Lollì, B., & Gasperini, P. (Eds.). (2016). CPTI15, the 2015 version of the parametric catalogue of Italian earthquakes. *Istituto Nazionale di Geofisica e Vulcanologia*. <https://doi.org/10.6092/INGV.IT-CPTI15>
- Rudolph, M. L., & Manga, M. (2010). Mud volcano response to the 4 April 2010 El Mayor-Cucapah earthquake. *Journal of Geophysical Research*, *115*, B12211. <https://doi.org/10.1016/j.marpetgeo.2009.01.019>
- Rudolph, M. L., & Manga, M. (2012). Frequency dependence of mud volcano response to earthquakes. *Geophysical Research Letters*, *39*, L14303. <https://doi.org/10.1029/2012GL052383>
- Rukavickova, L., & Hanzl, P. (2008). Mud volcanoes in the Khar Angalantyn Nuruu, NW Gobi Altay, Mongolia as manifestation of recent seismic activity. *Journal of Geosciences*, *53*, 181–189. <https://doi.org/10.3190/jgeosci.024>
- Snead, R. E. (1964). Active mud volcanoes of Baluchistan, West Pakistan. *Geographical Review*, *54*, 546–560. <https://doi.org/10.2307/212981>
- Stein, R. S. (1999). The role of stress transfer in earthquake occurrence. *Nature*, *402*, 605–609. <https://doi.org/10.1038/45144>
- Stein, S., & Wysession, M. (2003). *An introduction to seismology, earthquakes, and earth structure* (p. 498). Kundli, India: Blackwell Publishing.
- Stein, R. S., King, G. C. P., & Lin, J. (1992). Change in failure stress on the Southern San Andreas fault system caused by the 1992 magnitude = 7.4 Landers earthquake. *Science*, *258*, 1328–1332.
- Stewart, S. A., & Davies, R. J. (2006). Structure and emplacement of mud volcano systems in the South Caspian Basin. *AAPG Bulletin*, *90*, 771–786. <https://doi.org/10.1306/11220505045>
- Tinti, E., Scognamiglio, L., Michelini, A., & Cocco, M. (2016). Slip heterogeneity and directivity of the ML 6.0, 2016, Amatrice earthquake estimated with rapid finite-fault inversion. *Geophysical Research Letters*, *43*, 10,745–10,752. <https://doi.org/10.1002/2016GL071263>
- Toda, S., Stein, R. S., Richards-Dinger, K., & Bozkurt, S. (2005). Forecasting the evolution of seismicity in southern California: Animations built on earthquake stress transfer. *Journal of Geophysical Research*, *110*, B05S16. <https://doi.org/10.1029/2004JB003415>
- Toda, S., Stein, R. S., Sevilgen, V., & Lin, J. (2011). Coulomb 3.3 graphic-rich deformation and stress-change software for earthquake, tectonic, and volcano research and teaching—User guide. U.S. Department of the Interior. U.S. Geological Survey Open File Report 2011–1060 (63 pp.). Retrieved from <https://pubs.usgs.gov/of/2011/1060/>

- Tsunogai, U., Maegawa, K., Sato, S., Komatsu, D. D., Nakagawa, F., Toki, T., & Ashi, J. (2012). Coseismic massive methane release from a submarine mud volcano. *Earth and Planetary Science Letters*, *341*, 79–85. <https://doi.org/10.1016/j.epsl.2012.06.004>
- Van Der Elst, N. J., & Brodsky, E. E. (2010). Connecting near-field and far-field earthquake triggering to dynamic strain. *Journal of Geophysical Research*, *115*, B07311. <https://doi.org/10.1029/2009JB006681>
- Walter, T. R., Wang, R., Zimmer, M., Grosser, H., Lühr, B., & Ratdomopurbo, A. (2007). Volcanic activity influenced by tectonic earthquakes: Static and dynamic stress triggering at Mt. Merapi. *Geophysical Research Letters*, *34*, L05304. <https://doi.org/10.1029/2006GL028710>
- Wang, C.-Y., & Manga, M. (2010). Hydrologic responses to earthquakes and a general metric. *Geofluids*, *10*, 206–216. <https://doi.org/10.1111/j.1468-8123.2009.00270.x>
- Wells, D. L., & Coppersmith, K. J. (1994). New empirical relationships among magnitude, rupture length, rupture width, rupture area, and surface displacement. *Bulletin of the Seismological Society of America*, *84*, 974–1002.